

Probing the magnetic state of Fe/FeO/Fe trilayers by multiple isotopic sensor layers

S. Couet,^{1,a)} Th. Diederich,¹ S. Stankov,^{1,b)} K. Schlage,¹ T. Slezak,² R. Ruffer,³ J. Korecki,² and R. Röhlsberger¹

¹Deutsches Elektronen Synchrotron (DESY), Notkestraße 85, 22603 Hamburg, Germany

²Faculty of Physics and Applied Computer Science, AGH University Science and Technology, 30059 Krakow, Poland

³European Synchrotron Radiation Facility (ESRF), BP 220, 38043 Grenoble Cedex, France

(Received 10 March 2009; accepted 30 March 2009; published online 20 April 2009)

To obtain depth-selected information in magnetic multilayers, we propose a measurement scheme based on nuclear resonant scattering from multiple isotopic sensor layers. It takes advantage of the depth dependence of the photon wavefield intensity in grazing incidence geometry to enhance the signal from a given part of a multilayer. The technique is applied to study the magnetic structure of a Fe/Fe-oxide/Fe trilayer. We are able to fully determine in a direct manner the magnetic state of two ultrathin ⁵⁷Fe probe layers embedded in the system. The proposed technique can potentially be extended to various grazing incidence x-ray scattering methods. © 2009 American Institute of Physics. [DOI: 10.1063/1.3120770]

Multilayered magnetic structures are fundamental building blocks in a large variety of devices such as hard drives, magnetic random access memory, and magnetic field sensors.¹ In this class of systems, particular *interface coupling* phenomena (such as the exchange bias effect²) or *interlayer coupling* mechanisms modify the magnetic configuration of individual layers.¹ Understanding the integral properties of these systems requires a precise determination of the microscopic magnetic structure in a depth resolved manner where the magnetic configuration of individual layers is revealed.

Grazing incidence scattering techniques such as polarized neutron reflectometry or resonant x-ray reflectometry (which is sensitive to magnetism through dichroism effects) can be applied to investigate the magnetic and structural depth profile in multilayers.^{3–5} However, the magnetic depth profile extracted from data analysis is always the result of a modeling procedure. For complex magnetic structures incorporating layers of differing magnetic properties, it is often the case that several models of the magnetic depth profile could lead to the same reflectivity data.

Another approach to obtain magnetic depth profiles with subnanometer resolution is based on the isotope sensitive technique of nuclear resonant scattering (NRS) of synchrotron radiation, where isotopic probe layers are placed at selected positions in the layer system.⁶ Using this scheme, the depth resolution is given by the thickness of the isotopic probe layer used, which can be made as thin as a single atomic layer.⁷ In a NRS experiment, the time dependent de-excitation of the nucleus of the active isotope (in this case ⁵⁷Fe) is recorded after pulsed excitation using synchrotron radiation. The recorded temporal beat pattern (referred to as timespectrum) is a direct fingerprint of the configuration of the hyperfine split nuclear levels involved. The magnitude of

the hyperfine field (related to a given magnetic state) and its orientation (which is antiparallel to the atom's magnetic moment in the case of ⁵⁷Fe) can be precisely measured. The technique can be further used to determine the net magnetization of the layer⁸ and to study the formation and size of domains. The magnetic information encoded in the timespectrum is directly related to the magnetic state of the probe layer. If the probe layer is sufficiently thin, there is no need to model the depth dependent magnetic profile, and layer resolved magnetic information is obtained in a direct way. Most of the NRS experiments aiming at the determination of the magnetic structure were carried out using single probe layers.^{6,9} In this letter, we propose a simple measurement scheme that allows a complete and unique determination of the magnetic structure of two thin Fe layers magnetically coupled through a native oxide spacer layer. In order to study the magnetic state of the metallic Fe only (and eliminate the contribution of the magnetic oxide to the signal^{10,11}), we inserted an ⁵⁷Fe probe layer in both metal layers.

The NRS experiment was carried out in a dedicated ultra-high vacuum system¹² at the nuclear resonance beamline¹³ of the European Synchrotron Radiation Facility ESRF (France) ID18. The substrate is a flat W(110) single crystal which was cleaned by numerous cycles of annealing to 1500 K in an oxygen partial pressure of 1×10^{-7} mbar and flash annealed to 2100 K. Such procedure results in a clean and well ordered surface.¹⁴ A 2.4 nm thick ⁵⁶Fe layer is deposited via electron beam evaporation, with a 0.8 nm thick ⁵⁷Fe layer placed in its center (this isotopic substitution does not influence the chemical and magnetic properties of the layer), as depicted in Fig. 1(a). The low energy electron diffraction (LEED) pattern shows four bright spots resulting from the cubic symmetry of the surface. At this stage, a nuclear timespectrum was recorded in reflection geometry with the incidence angle of the x-ray beam set to 0.25°, above the critical angle of Fe at 14.4 keV (0.22°). The spectrum shows a single frequency beating which corresponds to a hyperfine field of 32.6 T, typical for ferromagnetic Fe at room temperature. The shape of the spectrum proves that the

^{a)}Present address: Instituut voor Kern-en Stralingsfysica, K.U.Leuven, Belgium. Electronic mail: sebastien.couet@fys.kuleuven.be.

^{b)}Present address: Institute for Synchrotron Radiation, Forschungszentrum Karlsruhe, Germany.

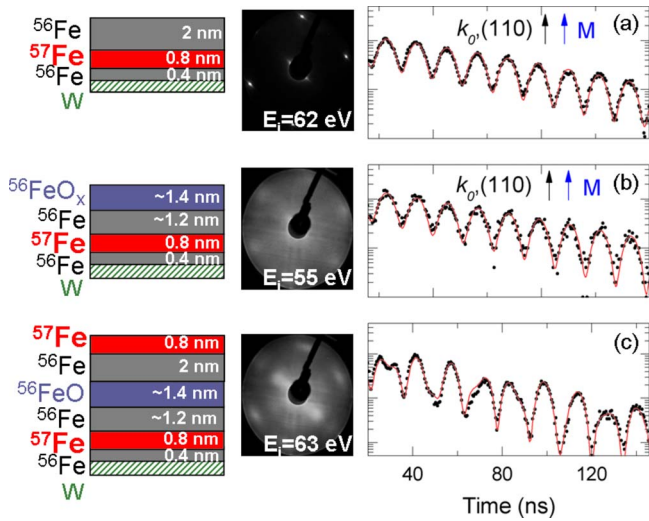


FIG. 1. (Color online) Growth of a Fe/native oxide/Fe trilayer incorporating two ^{57}Fe probe layers on a W substrate. The blurring of the LEED pattern in (b) and (c) documents the formation of a disordered oxide layer. The timespectrum of (a) and (b) shows that the magnetic moment of the ^{57}Fe probe layer is parallel to the (110) direction. In (c) the timespectrum indicates that the magnetic moment of at least one of the two probe layers is not collinear with the photon wavevector \vec{k}_0 .

layer is fully magnetized in the sample plane, parallel to the photon wavevector \vec{k}_0 and the (110) direction, most probably due to the strong cubic magnetocrystalline anisotropy of the epitaxial Fe film. The layer was subsequently oxidized by admission of molecular oxygen at a pressure of 1×10^{-5} mbar for 500 s. As seen in Fig. 1(b), the LEED pattern has a lower contrast due to the formation of a disordered oxide. The recorded timespectra does not change, meaning that the magnetic properties of the buried ^{57}Fe layer are not modified by the growth of the oxide. Finally, a second 2 nm ^{56}Fe layer is deposited with 0.8 nm of ^{57}Fe on its top. The LEED pattern shows faint diffraction spots meaning that the top Fe layer has a reduced crystalline quality. At this stage, the shape of the recorded timespectrum changes drastically compared to the single Fe layer, indicating that the magnetic moment in at least one of the two Fe layers is not collinear with the direction of the incident x-ray beam.

The recorded timespectrum is now a sum of the signals originating from the two probe layers. To disentangle the signals, we recorded timespectra at selected angles of incidence in the vicinity of the critical angle. This allowed us to tune the photon wavefield intensity at the position of the two ^{57}Fe probe layers, as sketched in Fig. 2. The normalized wavefield intensity $S(z)$ was calculated for selected angles following the formalism developed in Ref. 15. It is clearly seen that the wavefield intensity can be tuned to excite primarily one of the two, or both, layers. The recorded nuclear signal scales, as a result of the coherent scattering process, quadratically with the field intensity.¹⁵ Hence, the contributions from each layer will significantly depend on the angle of incidence θ , as depicted in the upper panel of Fig. 2. For example, at $\theta=0.1^\circ$, the ratio $S(z_1)^2/S(z_2)^2$ of the signal originating from the top probe layer compared to the lower probe layer is larger than 300. For $\theta=0.35^\circ$, the situation is reversed and $S(z_1)^2/S(z_2)^2=0.004$. At these angles, the scattered signal originates for more than 99% from one of the two probe layers. Because these field intensities can be cal-

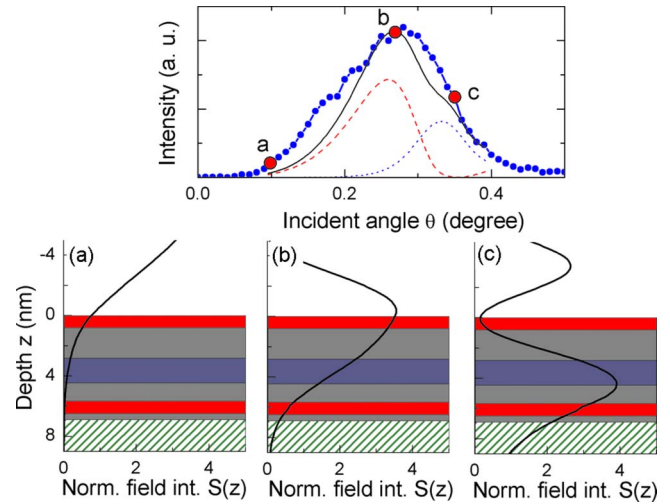


FIG. 2. (Color online) Upper panel: X-ray nuclear (integrated delayed intensity) reflectivity recorded near the critical angle on the Fe/Fe-oxide/Fe trilayer. The dashed and dotted lines are the square of the calculated field intensity $S(z)$ at the position of the top [$S(z_1)$] and bottom [$S(z_2)$] probe layers respectively. The solid line is the sum of both. Lower panel: Calculated wavefield intensity in the depth of the sample for the selected angles of incidence.

culated for a given structure, one can find immediately what will be the angles that give the best selectivity for the layer of interest.

These considerations apply to the timespectra recorded in a NRS experiment. Here, we recorded timespectra at the three incident angles shown in Fig. 2. At every angle, timespectra were taken along two azimuthal orientation separated by 45° : The (110) and the (100) in-plane direction of the lower Fe layer. As demonstrated by Schlage *et al.*,⁸ recording timespectra at different azimuthal angles of the sample allows one to unambiguously determine the net magnetization of the ^{57}Fe probe layers. All the timespectra were then consistently fitted using the CONUSS program.¹⁶ The result is shown in Fig. 3. The shape of the timespectrum changes drastically depending on which probe layer is primarily excited (i.e., depending on which incident angle θ is used). One sees that the spectrum recorded along the (110) direction and at $\theta=0.35^\circ$ is very similar to the spectrum of Fig. 1(a). This indicates that the magnetization of the lower ^{57}Fe layer did not change and is still aligned parallel to the easy axis. Quantitative analysis of the timespectra shows in

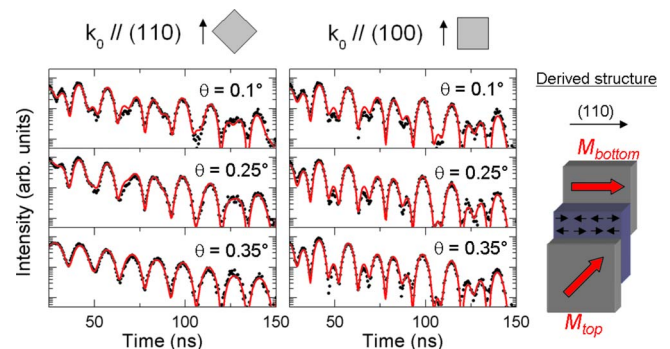


FIG. 3. (Color online) Set of timespectra recorded at three different angles of incidence θ for two different sample orientations. The red lines are consistent fits to determine unambiguously the magnetic structure of each probe layer. The right hand pictogram is the magnetic structure of the two probe layers (red arrow), as derived from the timespectra analysis.

fact that the top layer has the same hyperfine field of 32.6 T, while its magnetization is not collinear with the (110) direction and is canted by 45° in the sample plane. We can also derive from the consistent fitting of the data along the two azimuthal orientations of the sample that both layers are in a single domain state.

While the technique allows a direct determination of the magnetic structure (magnetic phase, domain state, and moment orientation) of the two Fe layers, it is difficult to conclude on the reason for the noncollinear alignment of the moments. For example, one can eventually expect that the different crystalline quality of the top layer results in an easy axis oriented 45° compared to the lower layer. However, it was also recently shown for polycrystalline Fe/FeO/Fe trilayers that a magnetic coupling appears between the Fe layers, which is mediated by an antiferromagnetically ordered oxide spacer.^{10,11} In these systems, the highly disordered oxide can also lead to coupling angles much lower than the nominal value of 90° , typical for this type of coupling mechanism.¹¹ These magnetically coupled systems also proved to sustain a single domain state throughout the magnetization reversal. This hypothesis therefore equally fulfills the experimentally observed magnetic structure.

In conclusion, we present a measurement scheme for the determination of the magnetic structure, domain state and moment orientation (also in and out of plane) in multilayers using NRS techniques and multiple probe layers. Proper tuning of the photon wavefield intensity allows to isolate the contribution of each probe layers to the signal. The method is applied to a coupled Fe/Fe-oxide/Fe trilayer, where a noncollinear, single domain magnetic structure is observed. Because no modeling of the depth dependent magnetic profile is needed, a unique solution is extracted from the consistent fitting procedure.

It should be mentioned that tuning the photon wavefield intensity can be used with other grazing incidence techniques such as grazing incidence small angle scattering or resonant techniques based on dichroism, to increase the coherently

scattered signal (and therefore the contrast) from a layer of interest (see, e.g., Ref. 17 for other applications).

The authors acknowledge the NRS group of the ESRF as well as M. Zajac and J. Meersschart for their precious help during the experiment. This work was supported by the European Commission under FP6 Contract No. NMP4-CT-2003-001516 DYNASYNC.

¹S. Parkin, X. Jiang, C. Kaiser, A. Panchula, K. Roche, and M. Samant, *Proc. IEEE* **91**, 661 (2003).

²J. Nogués and I. K. Schuller, *J. Magn. Magn. Mater.* **192**, 203 (1999).

³J. Meersschart, C. L'Abbé, F. M. Almeida, J. S. Jiang, J. Pearson, U. Welp, M. Gierlings, H. Maletta, and S. D. Bader, *Phys. Rev. B* **73**, 144428 (2006).

⁴V. Lauter-Pasyuk, H. J. Lauter, B. P. Toperverg, L. Romashev, and V. Ustinov, *Phys. Rev. Lett.* **89**, 167203 (2002).

⁵M. Hecker, S. Valencia, P. M. Oppeneer, H.-Ch. Mertins, and C. M. Schneider, *Phys. Rev. B* **72**, 054437 (2005).

⁶R. Röhlberger, H. Thomas, K. Schlage, E. Burkel, O. Leupold, and R. Ruffer, *Phys. Rev. Lett.* **89**, 237201 (2002).

⁷T. Slezak, M. Slezak, K. Matlak, R. Röhlberger, C. L'Abbé, R. Ruffer, N. Spiridis, M. Zajac, and J. Korecki, *Surf. Sci.* **601**, 4300 (2007).

⁸K. Schlage, R. Röhlberger, T. Klein, C. Strohm, E. Burkel, and R. Ruffer, *New J. Phys.* **11**, 013043 (2009).

⁹M. A. Andreeva, N. G. Monina, L. Häggström, B. Lindgren, B. Kalska, S. Kamali-M, S. N. Vdovichev, N. N. Salashchenko, V. G. Semenov, O. Leupold, and R. Ruffer, *Nucl. Instrum. Methods Phys. Res. B* **266**, 187 (2008).

¹⁰Th. Diederich, S. Couet, and R. Röhlberger, *Phys. Rev. B* **76**, 054401 (2007).

¹¹S. Couet, K. Schlage, Th. Diederich, R. Ruffer, K. Theis-Bröhl, K. Zhernenkov, B. Toperverg, H. Zabel, and R. Röhlberger, *New J. Phys.* **11**, 013038 (2009).

¹²S. Stankov, R. Ruffer, M. Sladeczek, M. Rennhofer, B. Sepiol, G. Vogl, N. Spiridis, T. Slezak, and J. Korecki, *Rev. Sci. Instrum.* **79**, 045108 (2008).

¹³R. Ruffer and A. I. Chumakov, *Hyperfine Interact.* **97**, 589 (1996).

¹⁴E. Partykajankowska, B. Sepiol, M. Sladeczek, D. Kmiec, J. Korecki, T. Slezak, M. Zajac, S. Stankov, R. Ruffer, and G. Vogl, *Surf. Sci.* **602**, 1453 (2008).

¹⁵R. Röhlberger, T. Klein, K. Schlage, O. Leupold, and R. Ruffer, *Phys. Rev. B* **69**, 235412 (2004).

¹⁶W. Sturhahn, *Hyperfine Interact.* **125**, 149 (2000).

¹⁷A. Gupta, D. Kumar, and C. Meneghini, *Phys. Rev. B* **75**, 064424 (2007).